

FCC Week 2019  
June 24<sup>th</sup>-28<sup>th</sup>  
Bruxelles



[www.cern.ch](http://www.cern.ch)



# 16 T magnet R&D overview

*Davide Tommasini*

On behalf of the EuroCirCol WP5

# Content

The talk summarizes the activity performed within EuroCirCol on the 16 T magnets, and will be composed of two parts.

The first part provides a general overview of the 16 T magnets programs and recall the related achievements of the EuroCirCol initiative, including new initiatives coming as a direct consequence of the program.

The second part, presented by Bernardo Bordini, will summarize the evolution and results of the EuroCirCol conductor program.

# Content

- Overview of 16 T magnet R&D
- EuroCirCol WP5
  - Impact in the magnets community
  - Contribution to the FCC CDR
  - Deliverable 5.4: a special contribution of the US Labs (US MDP) as EuroCirCol Partners
- Recent initiatives
  - Model magnets with CEA-CIEMAT-INFN
  - Chart-2
- Latest news
  - FCC 16 T program
  - US-MDP
- Evolution and results of the EuroCirCol Conductor Program (Bernardo Bordini)

# Overview of 16 T magnet R&D



**EuroCirCol WP5 (CEA, CERN, CIEMAT, UNIGENeva, KEK, INFN, TampereU, UTwente)**  
Feed the FCC CDR with design and cost model of 16 T magnets



**FCC 16 T Magnet Development**, supporting:

- conductor development & procurement
- R&D magnets and associated development
- model magnets



**US Magnet Development Program (ASC/NHMFL, BNL, FNAL, LBNL)**

- 14-15 T cosine-theta magnet (2017-2019)
- Design, manufacture, and test of a 2-layer 10 T CCT magnet
- Novel diagnostics and advanced modeling techniques

# EuroCirCol WP5 : impact in the community

- The program has set the parameters for conductor and magnets which are being used as a common reference worldwide. This has allowed/motivated different laboratories to work on the same basis.
- The existence of common targets has facilitated the promotion and development of parallel programs (in particular the US MDP, for both the conductor and the magnets).
- The choice of identifying certain strategic packages as a general support for the whole community (analysis tools, conductor characteristics, quench protection) has favoured interchange between labs.
- The existence of a reference framework has promoted and facilitated sharing of information, with an avalanche and contagious effect across generations, from students to senior scientists.
- A considerable effort has been put in place, by all parts, in cultivating this spirit through the whole duration of the program. In addition to meetings in person, visits to labs, conferences and workshops, the EuroCirCol WP5 has organized about 40 collaboration video-meetings and about 30 topical meetings, many of them with the enlarged participation of the US labs engaged in the US MDP.

# FCC CDR - 1

## Chapter 3

### Collider Technical Systems

#### 3.1 Overview

This chapter presents details of those technical infrastructure systems for which substantial research and development is required. It is known that it will be possible to scale up many systems from LHC for use in FCC-hh and these systems are not presented below. Various major systems such as magnets, cryogenics, RF, beam transfer and vacuum are described here as well as many smaller essential devices. Finally there is a description of the radiation environment in which they will have to perform. Details for all technical systems will be presented at a later stage in the design process but systems which require particular attention at this conceptual design stage have been identified and are presented here.

#### 3.2 Main Magnet System

##### 3.2.1 Introduction

The magnetic system of the FCC-hh will profit greatly from the experience gained with the LHC, which has demonstrated the feasibility and effectiveness of operating a large number of superconducting magnets cooled by using superfluid helium at 1.9 K. There will be about four times more magnets in FCC-hh than in LHC and the field amplitude produced by the arc dipoles will be increased by almost a factor of two, whilst maintaining a similar beam aperture and twin configuration. The field increase will be enabled by using Nb<sub>3</sub>Sn superconductor instead of the Nb-Ti used in the LHC arc dipoles. With respect to the conductor properties, the FCC-hh magnets will operate in a similar condition than the LHC magnets, with 14% margin on the load line and at about 60% of the maximum upper critical field B<sub>c20</sub>. It is believed that, with an appropriate R&D program, and if all magnets are cold tested before installation, this margin will be sufficient to achieve the nominal energy of the FCC-hh with limited magnet training. This technology, though not yet used in particle colliders, is being implemented for dipoles and quadrupoles of the HL-LHC project, where they will be operating at peak fields of between 11 and 12 T. One can expect that this technology will be ready to start mass production of 16 T magnets within a decade from the manufacture of a first long model.

##### 3.2.2 Superconducting Main Dipole

The main dipoles (MD) of the FCC are twin-aperture magnets of cosine-theta coil layout assembled in a helium-tight cold mass (CM) structure, integrated in a cryostat. A cross section of the system is presented in Fig. 3.1 and a 3D of the assembly is shown in Fig. 3.2.

The CM for the FCC MD is straight, and has a total length between the two extremities of the beam pipe flanges of 15.8 m and a magnetic length of 14.069 m. Its external diameter is 800 mm. It is

45

FCC-hh Conceptual Design Report

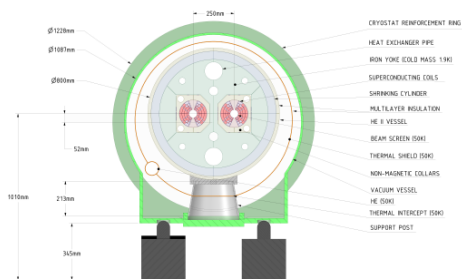


Figure 3.1: Main dipole cross-section.

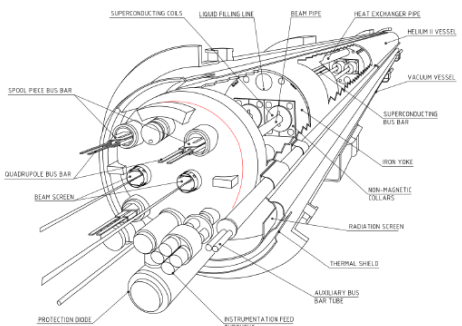


Figure 3.2: 3D-view of main dipole cold mass assembly.

installed in a cryostat structure composed of a radiation shield, a thermal screen and a vacuum vessel. It

46

PREPRINT submitted to Eur. Phys. J. ST

COLLIDER TECHNICAL SYSTEMS

is supported on three feet made from a composite material and a flange is bolted to the vacuum vessel.

All parts between the beam pipe and the shrinking cylinder, which defines the outer envelope of the cold mass, are immersed in superfluid helium at atmospheric pressure and cooled by a heat-exchanger tube, in which two-phase low-pressure helium circulates. The next temperature stage is that of the beam screen, cooled at a reference temperature of 50 K, which is also the temperature level for cooling the thermal screen and the support posts. The fact that the additional intermediate temperature level used in the LHC, in the range between 4 to 20 K, is missing, results in larger static losses from the cold mass and the support posts than in the LHC. The total heat loads of a cryodipole operating in steady state mode are estimated to be about 0.5 W/m at 1.9 K and about 10 W/m at 50 K. The target losses during a full cycle from nominal field, down to injection and up to nominal field again, which mainly come from the magnetisation of the superconductor, are set to 5 kJ/m at 1.9 K for the two apertures. The operating field of 16 T is generated by a current of 11441 A in a coil with a physical aperture of 50 mm. The distance between the axis of the two apertures is 250 mm. The magnet design is described in [163]. The main parameters of the MD, including the expected field quality, are listed in Table 3.1.

Table 3.1: Main dipole parameters.

Item	Unit	Value
Number of units		4668
Operating field	T	16.0
Coil physical aperture	mm	50.0
Operating current	A	11441
Operating temperature	K	1.9
Magnetic length @ 1.9K	mm	14069
Stored energy at 16 T (entire magnet)	MJ	37
Self-inductance at 16 T (entire magnet)	mH	570
Field margin on the load line at 16 T	%	14
Magnetisation losses (two apertures) over a full excitation cycle	kJ/m	5
Distance between aperture axes at 1.9K	mm	250
Number of coil turns per aperture		200
Surface of conductor (2 apertures)	cm <sup>2</sup>	131
Cold mass length beam pipe flange-to-flange at 1.9K	m	15.8
Mass of the cold mass	t	55
Mass of the cryostat	t	6
Geometric field harmonics b <sub>2</sub> , b <sub>3</sub> , b <sub>4</sub> , b <sub>5</sub>	units	3.7, -2.4, 0.95, 0.30
Contribution of persistent currents b <sub>20</sub> , b <sub>21</sub> , b <sub>22</sub> , b <sub>23</sub>	units	2.0, 23.0, 16.4, 9
Contribution of saturation b <sub>2</sub> , b <sub>3</sub> , b <sub>4</sub> , b <sub>5</sub>	units	-3.7, 2.5, -0.64, -0.11
Total field harmonics b <sub>2</sub> , b <sub>3</sub> , b <sub>4</sub> , b <sub>5</sub> at injection (1.06 T)	units	5.6, -25.0, 79.5, 2
Total field harmonics b <sub>2</sub> , b <sub>3</sub> , b <sub>4</sub> , b <sub>5</sub> at nominal field (16 T)	units	0.025, 0.11, 0.31, 0.18
Random harmonics b <sub>2</sub> , b <sub>3</sub> , b <sub>4</sub> , b <sub>5</sub>	units	0.93, 0.67, 0.47, 0.28
Random harmonics (skew) a <sub>2</sub> , a <sub>3</sub> , a <sub>4</sub> , a <sub>5</sub>	units	1.1, 0.75, 0.48, 0.33

The so called "margin on the load line" has been set to 14%, which is the same as the one adopted for the LHC at the nominal field of 8.3 T. Each MD aperture has 200 cable turns distributed in one upper and one lower pole, and each pole comprises two double layer (inner and outer) coils. Since the magnetic flux density varies considerably in the coil (it is much higher in the inner than in the outer pole), the design exploits the principle of grading (see below). The inner pole comprises 32 turns of a 0.5° keystoned Rutherford cable, made from 22 strands of 1.1 mm diameter, the outer pole has 68 turns of a 0.5° keystoned Rutherford cable, made from 38 strands of 0.7 mm diameter (see Table 3.3). The conductor distribution and the field amplitude in the coil is shown in Fig. 3.3, where one quarter of an

PREPRINT submitted to Eur. Phys. J. ST

47

FCC-hh Conceptual Design Report

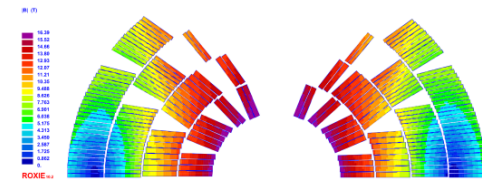


Figure 3.3: Conductor distribution and field amplitude in the coil (half aperture).

aperture is shown. The coil cross-section is asymmetric, to compensate the quadrupole component of the magnetic field coming from the interaction between the two magnet apertures.

The current density in the outer coil is larger than that in the inner coil because the two coils are connected in series and the cable in the inner layers has a larger conductor area than that in the outer layers. Thanks to grading, the current density, where the magnet field is lower, is increased, resulting in a considerable saving of conductor for a given margin on the load line. The structure is based on the so-called "key and bladders" concept together with the use of an aluminium cylinder surrounded by a stainless steel welded shell. The aluminium shell provides the increase of coil loading required from assembly to the operational temperature and during magnet powering. The stainless shell, as well as adding stiffness to the structure, provides helium tightness, alignment fiducials and support for the magnet end covers. The CM assembly and its main components are shown in Fig. 3.4.

The field distribution in the magnet cross section for a central field in the magnet aperture of 16 T, is shown on the left side of Fig. 3.5. The von Mises stress distribution in the structure at the same field of 16 T is shown on the right side of the same picture. The detail of the stress distribution in the coil cross section is shown in Fig. 3.6. Concerning the electromagnetic section, the ferromagnetic yoke is saturated, thus producing a stray field which is about 0.1 T at the boundary of a non-magnetic cryostat. Concerning the structural section, the coil remains entirely under azimuthal compression (with a minimum pressure of 6 MPa) up to the 16 T field amplitude. In these conditions the peak stress on the coil does not exceed 180 MPa. The stress in the other part of the structure remains well below the limits of the magnet components.

Each magnet will be cold tested prior to installation in the tunnel. Depending on its training performance, the magnet may also be submitted to a thermal cycle to confirm that, once installed, the magnet can be powered up to nominal field without experiencing training quenches. As was successfully done for the LHC, a warm-cold magnet measurement correlation will be established, based on the statistics from pre-series magnets. All series magnets will be then magnetically measured warm. Only a small percentage of them will also be measured at operating (cryogenic) temperatures.

##### 3.2.3 Field Quality

The field error naming convention follows the one adopted for the LHC [164]. The systematic field error values are deterministic and computed with ROXIE: they comprise a geometric contribution, a contribution coming from persistent currents and the effect of saturation of the ferromagnetic yoke. The contribution from the persistent currents [165] has been computed using the conductor parameters of Table 3.2 and assuming that artificial pinning has been implemented which allows the critical current

48

PREPRINT submitted to Eur. Phys. J. ST

# FCC CDR - 2

## COLLIDER TECHNICAL SYSTEMS

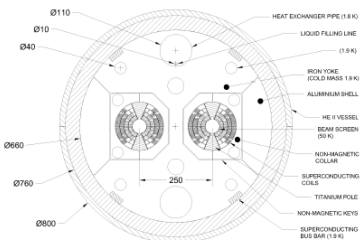


Figure 3.4: Main dipole cold mass.

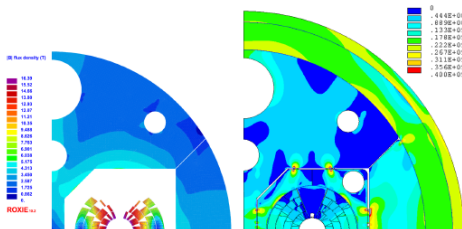


Figure 3.5: Electromagnetic (left) and structural (right) cross-section for a central field of 16 T.

(thus the magnetisation) to be reduced at low fields. Considering that it is very unlikely that a perfect point pinning can be achieved, the contribution reported in Table 3.1 has been obtained considering 50% of perfect point pinning. The random values are due to the spread of the geometric and persistent current contributions. The geometric random errors have been determined by means of Monte-Carlo simulations which include a random displacement of the coil blocks with a root-mean-square (RMS) amplitude

## FCC-hh Conceptual Design Report

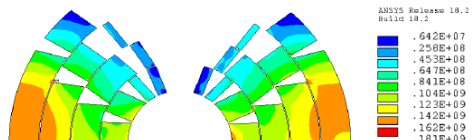


Figure 3.6: Stress distribution (von Mises) in the coil for a central field amplitude of 16 T.

$d = 50 \mu\text{m}$ . The uncertainty errors are linked to the production line. At this stage, it is assumed, as for HL-LHC, that the production is uniform; therefore the uncertainties are equal to the random values. Further optimisation is on-going to passively correct the  $b_1$  error from persistent currents by using iron shims. The yoke shape will also be further optimised to minimise the saturation effects.

### 3.2.4 Magnet Protection

The magnet and its protection system are conceived to limit the hot spot temperature to below 350 K in the case of a quench and the peak voltage to ground in the coil below 2.5 kV. This voltage limit includes up to 1.2 kV due to the quench evolution in the magnet itself and up to 1.3 kV from the circuit. The protection system can be based on the coupling-loss-induced quench method (CLIQ), on quench-heaters alone or on a combination of both. On paper, all options effectively protect the magnets within the above limits [166]. Experiments on FCC models and prototypes will show if CLIQ can be implemented in real conditions with the required reliability and redundancy for every quench situation. For the reasons above, though it is believed that CLIQ has the potential to quench the entire magnet in 30 ms after the initiation of a quench (time delay), the 16 T magnets have been designed assuming a time delay of 40 ms, which is compatible with the use of quench-heaters.

### 3.2.5 Other Design Options

In addition to the baseline design of the cosine-theta coil type, other design options have been studied in detail; they will be tested experimentally in the coming years. These other designs are the block-type [167], the common-coil [168] and the canted-cosine-theta (CCT) [169] configurations. All options have been explored considering the same assumptions, in particular concerning the magnet aperture (50 mm), the field amplitude (16 T), the conductor performance (assuming the availability of a conductor with a target critical current density of  $1500 \text{ A/mm}^2$  @ 4.2 K @ 16 T, corresponding to  $2300 \text{ A/mm}^2$  @ 1.9 K @ 16 T), the margin on the load line (9-14%) and the allowed mechanical constraints on the superconducting coil (<150 MPa at warm and <200 MPa at cold). The electromagnetic cross section of each of these options is shown in Fig. 3.7. Their salient features, with respect to the baseline cosine-theta, are shown in Table 3.2.

Each of these alternatives features some interesting characteristics which may have a potential to become competitive to the baseline cosine-theta design in terms of performance, in particular if they would allow operation at a lower margin on the load-line, thus reducing the required amount of conductor.

### 3.2.6 Low Temperature Superconductors

The 16 T dipole magnets for the FCC rely on  $\text{Nb}_3\text{Sn}$ . Experience has been gained in the use of this technology in both the US and Europe, not only on R&D magnets but, more recently also on accelerator

## COLLIDER TECHNICAL SYSTEMS

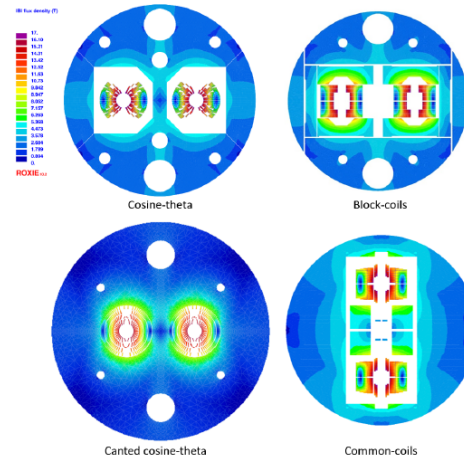


Figure 3.7: Electromagnetic cross sections of the 16 T dipole design variants.

magnets, thanks to the HL-LHC project. Both the electrical performance and filament size are currently beyond state-of-the-art for  $\text{Nb}_3\text{Sn}$  wire. A dedicated R&D programme has been launched worldwide, with some promising results already [170]. This programme has three phases. In the first phase, the focus is on increasing the critical current by 50% with respect to HL-LHC ( $1500 \text{ A/mm}^2$  at 4.2 K and 16 T), maintaining high RRR (150). This requires a major breakthrough and work on novel methods, such as artificial pinning centres (APC), grain refinement and architectures. In the second phase, the conductor will be optimised to reduce the magnetisation, in particular at low fields, by modifying the effective filament diameter and possibly using APC. The third phase can be considered the preparation to industrialisation, focusing on achieving long unit lengths (5 km) and competitive cost (5 kEuro/kAm at 4.2 K and 16 T). As reported in [170], despite the short time since the start of the program, high-performing  $\text{Nb}_3\text{Sn}$  conductors have been already produced by new collaborating partner institutes and companies, achieving a  $J_c$  performance of the order of the specification for HL-LHC. Work performed on grain refinement and APC has shown promising results, nearly doubling the  $J_c$  at 12 T, 4.2 K on small samples. Finally, to improve the training of magnets, the introduction of materials with high heat

## FCC-hh Conceptual Design Report

Table 3.2: Salient features of design options for 16 T magnets.

Parameter	Cos-theta	Block-coil	CCT	Common-coil
Peak field on conductor [T]	16.40	16.73	16.35	16.57
Operating current [A]	11441	10176	18135	15880
Inductance @ 16 T [mH/m]	38	48	18	26
Outer yoke diameter [mm]	660	616	750	650
Mass of conductor [kg/m]	115	120	148	145

capacity ( $\text{Gd}_2\text{O}_3$ ) directly within the  $\text{Nb}_3\text{Sn}$  wire is being considered.

Two distinct conductors are used for the 16 T dipoles: a high-field (HF) conductor used for the inner pole and a low-field (LF) conductor used for the outer pole. The parameters of the HF and LF conductors are summarised in Table 3.3. It is assumed that the insulated conductor can be subjected to pressures of up to 150 MPa at ambient temperature and 200 MPa when cold, without experiencing an irreversible degradation. Based on the information coming from tailored experiments and from magnet tests, these values are considered to be challenging but realistic. Finally, due to the high  $J_c$ , the large filament diameter and the large amplitude of a magnet cycle, the magnetisation losses of these magnets have a considerable impact on the design of the cryogenic system, which assumes 5 kJ/m at 1.9 K for the two apertures. This limit can be respected with filament diameters of around  $20 \mu\text{m}$  and if new manufacturing techniques have been developed, e.g. the aforementioned APC, and if the reset current during the machine powering cycle will be optimised.

Table 3.3: Target parameters for the main dipole conductor.

Property	Unit	Value
<b>Wire</b>		
Critical current density at 16 T and 1.9 K	$\text{A/mm}^2$	1500
Strand diameter HF conductor	mm	1.1
Strand diameter LF conductor	mm	0.7
Filament size HF conductor	$\mu\text{m}$	20
Filament size LF conductor	$\mu\text{m}$	20
Cu/iron/Cu HF conductor		0.8:1
Cu/iron/Cu LF conductor		2:1:1
<b>Cable</b>		
Number of strands HF cable		22
Number of strands LF cable		38
Width of HF cable	mm	13.2
Width of LF cable	mm	14.0
Keystone angle of HF/LF cable	degrees	0.5
Average thickness of HF cable	mm	1.950
Average thickness of LF cable	mm	1.265

### 3.2.7 Superconducting Main Quadrupole

The main quadrupoles (MQ) of FCC are twin-aperture magnets based on a cosine-theta coil configuration assembled in a 20 mm thick helium II vessel. Their design is detailed in [171]. The cooling system and the cryogenic features in the iron yoke are linked to the MQ magnet characteristics. Like the MQ magnet, the inter-beam distance is 250 mm and the physical aperture is 50 mm in diameter. Each aperture is mechanically independent from the other due to the use of a collar-and-key mechanical assembly. The

# FCC CDR - 3

main parameters of the MQ are listed in Table 3.4. Each double pancake is made of 18 turns of Nb<sub>3</sub>Sn Rutherford cable with a 0.4° keystone angle. The cable consists of 35 strands, 0.85 mm in diameter, the filament size is 20 μm. The CLIQ system protects the magnet with a hot spot limited to 350 K and a peak voltage to ground below 900 V.

Table 3.4: Main quadrupole parameters.

Item	Unit	Value
Number of units		744
Operating gradient	T/m	367
Coil physical aperture	mm	50.0
Peak field	T	10.51
Operating current	A	22500
Operating temperature	K	1.9
Magnetic length @ 1.9K	mm	7063
Stored energy at 16 T (entire magnet)	MJ	3.7
Self-inductance at 16 T (entire magnet)	mH	14.4
Field margin on the load line at nominal	%	20
Temperature margin at nominal	K	4.6
Distance between aperture axes at 1.9K	mm	250
Number of coil turns per aperture		72
Mass of the cold mass	t	17
Total field harmonics at nominal $b_0, b_{10}$	units	-0.47, 0.41
Total field harmonics at injection $b_0, b_{10}$	units	-22.3, 2.40

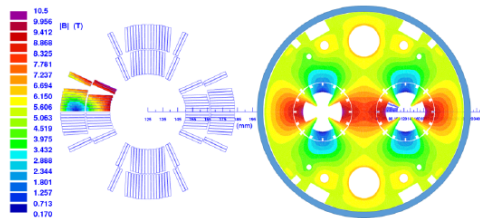


Figure 3.8: Left: Conductor distribution and magnetic field [T] in the coil. Right: iron yoke, steel collar layout and Hell vessel.

### 3.2.8 Other Magnets in the Arcs

For the FCC-hh, the FODO cell length in the arc was chosen to be 213 m, roughly double the length of the LHC FODO cell. The FCC-hh has 8 long arcs, each with 36.5 FODO cells, and 4 short arcs, each with 15 FODO cells. Each FODO cell has 12 dipoles and 2 Short Straight Sections (SSS). As in the LHC, each SSS contains one MQ, and sextupole (MS) and dipole corrector magnets (MC). Depending on the

SSS location in the arc, there may be in addition octupole corrector magnets (MO), tuning quadrupoles (MQT) or skew quadrupoles (MQS). It is planned to have 3510 MB-MB, 704 MB-SSS and 704 SSS-MB interconnections in the arcs. The magnet types and their main parameters are listed in Table 3.5. All these magnets, except the DIS quadrupole (MQDA), use Nb-Ti technology. The MQDA relies on Nb<sub>3</sub>Sn. The space required for the interconnections and the magnet extremities is summarised in Table 3.6, which shows the target distance between the magnetic ends of the different magnets.

Table 3.5: Other magnets in the Arcs.

Magnet type	Technology	Number	Strength	Length
Lattice sextupoles (MS)	NbTi	696	7000 T/m <sup>2</sup>	1.2 m
Lattice octupoles (MO)	NbTi	480	200000 T/m <sup>3</sup>	0.5 m
Dipole correctors (MCB)	NbTi	792	4 T	1.2 m
Trim quadrupoles (MQT)	NbTi	120	220 T/m	0.5 m
Skew quadrupoles (MQS)	NbTi	96	220 T/m	0.5 m
MCS	NbTi	2x4668	3000 T/m <sup>2</sup>	0.11 m
DIS quadrupole (MQDA)	Nb <sub>3</sub> Sn	48	360 T/m	9.7 m
DIS trim quadrupole (MQTL)	NbTi	48	220 T/m	2.0 m

Table 3.6: Distances between magnets (magnetic lengths).

Magnet types	Distance (m)	Remarks
MB-MB	1.5	For 0.11 m long MCS
MB-BPM	1.3	BPM stands for beam position monitor
MQ-other	0.35	Other magnetic elements in SSS
Other-other	0.35	

### 3.2.9 Low-beta Triplets

The low-beta triplets are composed of quadrupole magnets and corrector magnets. There are two types of low-beta triplets for installation in the high- and low-luminosity interaction regions, respectively. The magnet types and their main parameters are listed in Table 3.7. The target distance between the magnetic length of each of these magnets is two metres, ignoring the corrector magnets.

Table 3.7: Low-beta Triplets.

Magnet type	Technology	Number/IP	Strength	Length	Aperture
Q1 high lumi	Nb <sub>3</sub> Sn	4	130 T/m	14.3 m	164 mm
Q2 high lumi	Nb <sub>3</sub> Sn	8	105 T/m	12.5 m	210 mm
Q3 high lumi	Nb <sub>3</sub> Sn	4	105 T/m	14.3 m	210 mm
Q1 low lumi	Nb-Ti	4	270 T/m	10.0 m	64 mm
Q2 low lumi	Nb-Ti	4	270 T/m	15.0 m	64 mm
Q3 low lumi	Nb-Ti	4	270 T/m	10.0 m	64 mm

The magnets around the collision points will be exposed to high radiation levels which may adversely affect their performance. It is assumed that the conductor performance can be maintained until a displacement-per-atom (DPA) value of  $2 \times 10^{-5}$ , and that the magnet insulation can withstand an accumulated radiation dose of 30 MGy. These values may be exceeded over the machine lifetime, going up to 40 to 50 MGy assuming the use of the baseline 35 mm thick tungsten shield. Some optimisation to reduce this value in the collision optics is ongoing. This radiation load may be still affordable if either a more

radiation resistant impregnation system is developed in the magnets or if the triplet magnets are replaced once in the machine lifetime. Furthermore, the estimated static heat load using the baseline shield and at the nominal operation conditions, is 4.5 mW/cm<sup>2</sup>, which corresponds to a temperature increase of the coil of about 0.5 K.

### 3.2.10 Other Magnets

Depending on their location, the matching and dispersion suppressor quadrupoles have a cross section similar to the MQ but with apertures increased to up to 70 mm. Around 156 matching quadrupoles are distributed as follows: 96 in the dispersion suppressors, 16 in the high-luminosity experiment insertions, 20 in the low-luminosity experiment insertions and injections, 6 in the injection and extraction sections, 8 in the RF section and 10 in the collimation section. Furthermore, 48 trim quadrupoles are installed in the 16 dispersion suppressors. The same type of magnets as those in the LHC are required in the collimation insertion. However, the radiation load in the betatron collimation region is large. Normal-conducting dipole magnets with bedstead coils are proposed in order to reduce the radiation dose by one order of magnitude compared to magnets with racetrack coils. Finally, there are 12 normal-conducting and 8 superconducting separation and recombination dipoles. These magnets are listed in Table 3.8.

Table 3.8: Other magnets.

Magnet type and location	Tech	Number	Strength	Length	Aperture
Separation dipoles D1 high lumi	Copper	6/IP	1.91 T	3×12.5 m	168 mm
Recombination dipoles D2 high lumi	Copper	6/IP	1.91 T	3×12.5 m	58 mm
Separation dipoles D1 low lumi	Nb <sub>3</sub> Sn	4/IP	12 T	12.5 m	100 mm
Recombination dipoles D2 low lumi	Nb <sub>3</sub> Sn	4/IP	10 T	15.0 m	60 mm
Q4 high lumi	Nb-Ti	2/IP	175 T/m	9.1 m	70 mm
Q5 high lumi	Nb-Ti	2/IP	260 T/m	12.8 m	60 mm
Q6 high lumi	Nb-Ti	2/IP	225 T/m	12.8 m	60 mm
Q7 high lumi	Nb <sub>3</sub> Sn	4/IP	400 T/m	14.3 m	50 mm
Q4 low lumi	Nb-Ti	2/IP	200 T/m	9.1 m	70 mm
Q5 low lumi	Nb-Ti	2/IP	275 T/m	12.8 m	50 mm
Q6 low lumi, extraction side	Nb-Ti	1/IP	170 T/m	12.8 m	50 mm
Q6 low lumi, injection side	Nb-Ti	2/IP	170 T/m	9.1 m	70 mm
Q7 low lumi	Nb-Ti	2/IP	84 T/m	12.8 m	50 mm
Q8 low lumi	Nb-Ti	2/IP	120 T/m	9.1 m	70 mm
MCB2 (single ap) high lumi	Nb-Ti	8	3 T HV	1.3 m	240 mm
MCB3 (single ap) high lumi	Nb-Ti	4	3 T HV	1.3 m	240 mm
MCB4 high lumi	Nb-Ti	4	3 T	3 m	70 mm
MCB4v high lumi	Nb-Ti	4	3 T	3 m	70 mm
Orbit Correctors low lumi	Nb-Ti	12	3 T	1 m	64 mm

### 3.3 Cryogenic Beam Vacuum System

#### 3.3.1 Overview

Vacuum stability at cryogenic temperature is a key element for the design of the hadron collider. Significant levels of synchrotron radiation are produced in this machine that result in heat power depositions of the order of 30 W/m. Early analysis has revealed that it is unlikely to be able to design a beamscreen akin to the one in the LHC that can cope with the operation conditions. A novel design is needed that can effectively shield the cold bore of the superconducting magnets operating at 1.9 K from the heat load. The concept must also help mitigating electron cloud, resistive and impedance effects from the



# Deliverable 5.4: a contribution of the US MDP



Manufacturing folder for reference design dipole short

EUROCIRCOL-P3-WP5-D5.4

Date: 20/03/2019

Grant Agreement No: 654305

## EuroCirCol

European Circular Energy-Frontier Collider Study

Horizon 2020 Research and Innovation Framework Programme, Research and Innovation Action

### DELIVERABLE REPORT

## MANUFACTURING FOLDER FOR REFERENCE DESIGN DIPOLE SHORT MODEL

Document identifier:	EuroCirCol-P3-WP5-D5.4 EDMS 2041779
Due date:	End of Month 46 (April 1, 2019)
Report release date:	26/03/2019
Work package:	WP5 (High-field accelerator magnet design)
Lead beneficiary:	CERN
Document status:	IN WORK (V0.2)

#### Abstract:

Manufacturing folder for a novel high-field cosine-theta model magnet, suitable for the hadron collider designed in the scope of the EuroCirCol project, which is part of the international Future Circular Collider study.

Grant Agreement 654305

PUBLIC

1 / 8



Manufacturing folder for reference design dipole short model

EUROCIRCOL-P3-WP5-D5.4

Date: 20/03/2019

## 1. INTRODUCTION

The specifications and parameters, set by the EuroCirCol WP5, have been implemented in the engineering design of a cos-theta dipole model magnet developed by Fermilab in the framework of the US Magnet Development Program (MDP), which includes Fermilab, LBNL, NIMFEL and recently BNL. The magnet design and manufacturing has been in part adapted to the tooling used for the 11 T dipole for the HL-LHC upgrade project, which was available at FNAL when the activity started.

The status of advancement of the model magnet is well beyond the initial goal of EuroCirCol, going beyond the delivery of a manufacturing folder. At the time of the writing of this report all magnet parts have been manufactured and the magnet is assembled and ready for testing (Fig.1).



Fig.1 The cos-theta dipole model magnet with project leader A.V. Zlobin and his team (FNAL).

Grant Agreement 654305

PUBLIC

4 / 8



Manufacturing folder for reference design dipole short model

EUROCIRCOL-P3-WP5-D5.4

Date: 20/03/2019

## 2. MAGNET PARAMETERS

The magnet is based on a 4-layer graded cos-theta coil with 60 mm aperture and cold iron yoke. To counteract the large Lorenz forces, a novel mechanical structure based on a vertically split iron yoke, locked by large aluminum I-clamps and supported by a thick stainless steel skin, has been developed at FNAL.

The main magnet parameters are summarized in Table 1.

Table 1: main parameters of the cos-theta model magnet.

Parameter	Unit	Value
Magnet free aperture	mm	60
Bore field at short sample limit @ 1.9 K	T	17.0
Peak field at short sample limit @ 1.9 K	T	17.7
Current at short sample limit @ 1.9 K, I <sub>c</sub>	kA	12.5
Inductance at I <sub>c</sub>	mH/m	26
Number of cable strands (Cable1/Cable2)		28/40
Cable width (Cable1/Cable2) after reaction	mm	15.10/15.10
Cable mid-thickness (Cable1/Cable2) after reaction	mm	1.870/1.319

## 3. MANUFACTURING FOLDER

The manufacturing folder is composed of the following drawings.

- F10050785\_15T Assembly
- F10050871\_I-clamp
- F10050291\_Iron Lamination
- F10047874\_Coil assembly
- F10055320\_Coil L1-2
- F10055321\_Coil L3-4
- F10047809\_L1 Pole LE
- F10047844\_L1 Pole RE
- F10048996\_L2 Pole LE
- F10049080\_L2 Pole RE
- F10054821\_L1 Splice Block
- F10054822\_L2 Splice Block
- F10052356\_L1 Wedge
- F10052369\_L2 Wedge
- F10047811\_L1 Spacer1 LE
- F10047813\_L1 Spacer2 LE
- F10047825\_L1 Spacer3 LE
- F10047843\_L1 Spacer4 LE
- F10047863\_L1 Spacer1 RE
- F10047864\_L1 Spacer2 RE
- F10049005\_L2 Spacer1 LE
- F10049010\_L2 Spacer2 LE
- F10049011\_L2 Spacer3 LE

Grant Agreement 654305

PUBLIC

5 / 8

# Recent initiatives : model magnets

As a spin-off of EuroCirCol, the work developed in WP5 will be continued and exploited in the design, manufacture and test of model magnets. The activity is supported by National Institutes and by the CERN FCC 16 T program.

## ADDENDUM FCC-GOV-CC-0121 / KE3782/TE

The European Organization for Nuclear Research ("CERN"), an Intergovernmental Organization having its seat at Geneva, Switzerland, and the Commissariat à l'énergie atomique et aux énergies alternatives ("CEA"),	
This Addendum defines a contribution by a Participant under Article 6 of the Memorandum of Understanding for the FCC Study (FCC-GOV-CC-0004/MS 1390795).	
Address:	Centre CEA Paris Saclay Groscurieux 91115 Ardenne, France Supplier's code: CEA-01, Address code: SC02 Budget code: 10832
<b>SCOPE OF WORK</b>	
The development of magnets for the FCC requires the demonstration of Nb <sub>3</sub> Sn accelerator magnets with performances far beyond the HiLumi targets with 50 mm coil aperture. This work follows-up on the Nb <sub>3</sub> Sn high-field development program started at CEA with the participation in the design and construction of FRESCA2 dipole magnet. It covers the realization of a FCC-hh short dipole model magnet designed within the H2020 EuroCirCol design study and the conceptual design of the FCC-hh arc quadrupole magnet.	

Thursday 15:30-17:00  
High-field magnet R&D  
The CEA dipole model for the FCC (Etienne Rochepault)

## ADDENDUM FCC-GOV-CC-0130 / KE3920/TE

THE EUROPEAN ORGANIZATION FOR NUCLEAR RESEARCH (hereinafter referred to as "CERN"), an Intergovernmental Organization having its seat at Meyrin CH-1211, Geneva 23, Switzerland, represented by Frédéric Bordry, Director for Accelerators and Technology,
THE CENTER FOR THE DEVELOPMENT OF INDUSTRIAL TECHNOLOGY, E.I.C.E. (hereinafter referred to as "CDTI"), a Spanish public entity, created by R.D.-Ley 8/1995 of 30th November, established in C/ Cid n. 4, 28001 Madrid, Spain, duly represented by Javier Ponce Martínez, Director-General, and
THE CENTER FOR RESEARCH ON ENERGY, ENVIRONMENT AND TECHNOLOGY, O.A. M.P. (hereinafter referred to as "CIEMAT"), a Spanish public entity with registered office at Avenida Complutense, 40, 28040 Madrid, duly represented by Rafael Rodrigo Montero, President, as stipulated in Article 8, R.D. 1502/2000, 1 of December, which approved the Statutes of CIEMAT, (hereafter individually referred to as the "Contributor" and jointly as the "Contributors"),

Just signed

## ADDENDUM No. KE4102/FCC

to  
FCC Memorandum of Understanding (FCC-GOV-CC-0004/17.10.2014)  
between  
THE EUROPEAN ORGANIZATION FOR NUCLEAR RESEARCH (CERN)  
and  
THE ISTITUTO NAZIONALE DI FISICA NUCLEARE ("INFN")  
concerning  
Collaboration on 16 T - Nb<sub>3</sub>Sn Short Model Magnet Production  
in the framework of the FCC Study hosted by CERN

Thursday 15:30-17:00  
High-field magnet R&D  
The INFN dipole model for the FCC (Riccardo Valente)

# Recent initiatives : Chart-II, 2019-2023

## Mission:

- Develop a Swiss-based expertise in applied superconductivity and superconducting magnets for HEP, in view of a possible FCC-hh or HE-LHC.

## Focus on:

- High field magnets R&D (both LTS and HTS)
- Particle collider design (beam dynamics, collimation, materials at extreme conditions)
- Advanced acceleration methods (high gradient THz Laser Acceleration)

## High-field magnets:

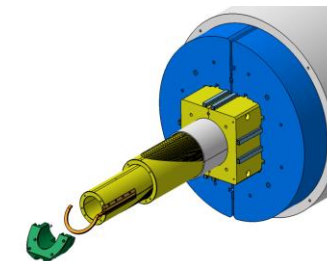
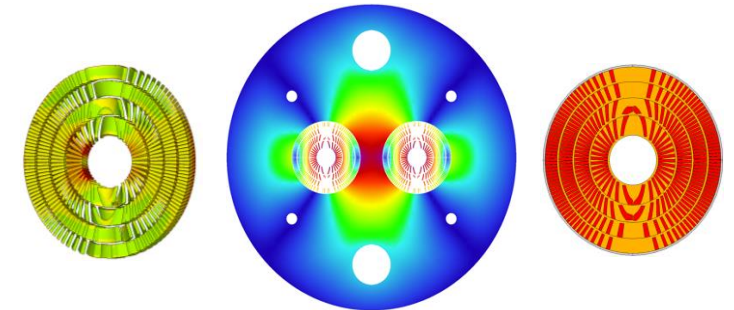
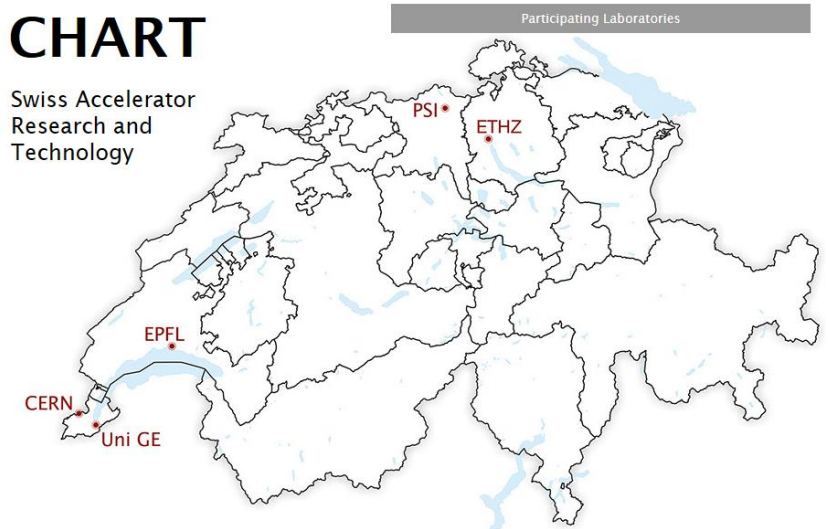
- Establish the infrastructure needed to build and test SC accelerator magnets
- Design, build, and test superconducting-magnet models according to needs of the FCC design study:
  - explore CCT technology for Nb<sub>3</sub>Sn 16-T dipoles,
  - develop up to 2-m-long high-field prototypes – not necessarily of CCT type
  - contribute to HTS accelerator-magnet R&D constructing technology models

## Other HTS magnets:

- Design, build, and test a HTS variant of the SLS 2.0 super-bend magnet.
- Design, build, and test several periods of an HTS undulator magnet.

## CHART

Swiss Accelerator  
Research and  
Technology



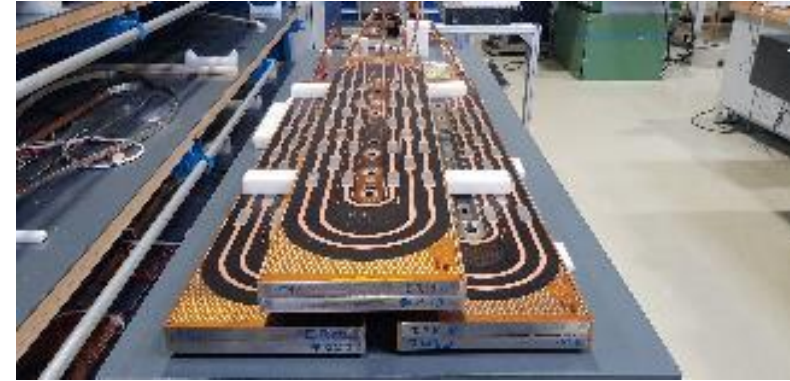
# FCC 16 T Magnet Development: latest news

eRMC magnet structure was assembled using instrumented aluminium dummy coils



Two thermal cycles, using 2 different interference level, were used to characterise the mechanical structure behaviour at cryogenic temperature

Three coils were produced and are ready for assembly



The magnet will be assembled using 2 coils and the first cold powering tests are scheduled before end 2019

# US MDP: latest news



**Thursday 15:30-17:00 : High-field magnet R&D**

The US-MDP program (S.Prestemon)

The US-MDP costheta model (A.V.Zlobin)

# Evolution and results of the EuroCirCol Conductor Program

Thank you for your attention

